THE JOURNAL OF BIOLOGICAL CHEMISTRY VOL. 285, NO. 31, pp. 23676–23686, July 30, 2010
© 2010 by The American Society for Biochemistry and Molecular Biology, Inc. Printed in the U.S.A.

A Conserved Aspartate Determines Pore Properties of Anion Channels Associated with Excitatory Amino Acid Transporter 4 (EAAT4)*[S]

Received for publication, March 24, 2010, and in revised form, May 30, 2010 Published, JBC Papers in Press, June 2, 2010, DOI 10.1074/jbc.M110.126557

Peter Kovermann[‡§1], **Jan-Philipp Machtens**[‡§], **David Ewers**[‡§], **and Christoph Fahlke**[‡§]

From the [‡]*Institut für Neurophysiologie, Medizinische Hochschule, D-30625 Hannover, Germany and the* [§]*Zentrum für Systemische Neurowissenschaften, D-30559 Hannover, Germany*

Excitatory amino acid transporter (EAAT) glutamate transporters function not only as secondary active glutamate transporters but also as anion channels. Recently, a conserved aspartic acid (Asp^{112}) within the intracellular loop near to the end of transmembrane domain 2 was proposed as a major determinant of substrate-dependent gating of the anion channel associated with the glial glutamate transporter EAAT1. We studied the corresponding mutation (D117A) in another EAAT isoform, EAAT4, using heterologous expression in mammalian cells, whole cell patch clamp, and noise analysis. In EAAT4, D117A modifies unitary conductances, relative anion permeabilities, as well as gating of associated anion channels. EAAT4 anion channel gating is characterized by two voltage-dependent gating processes with inverse voltage dependence. In wild type EAAT4, external L-glutamate modifies the voltage dependence as well as the minimum open probabilities of both gates, resulting in concentration-dependent changes of the number of open channels. Not only transport substrates but also anions affect wild type EAAT4 channel gating. External anions increase the open probability and slow down relaxation constants of one gating process that is activated by depolarization. D117A abolishes the anion and glutamate dependence of EAAT4 anion currents and shifts the voltage dependence of EAAT4 anion channel activation by more than 200 mV to more positive potentials. D117A is the first reported mutation that changes the unitary conductance of an EAAT anion channel. The finding that mutating a pore-forming residue modifies gating illustrates the close linkage between pore conformation and voltage- and substrate-dependent gating in EAAT4 anion channels.

Glial and neuronal excitatory amino acid transporters (EAATs)[2] remove glutamate from the synaptic cleft to ensure low resting glutamate levels and to prevent neuronal damage by excessive glutamate receptor activation. EAATs are not only secondary active glutamate transporters but also anion-selective channels (1). For some EAAT isoforms, anion currents are much smaller than electrogenic uptake currents. For other isoforms, anion currents represent the predominant transporter-mediated current component (2–5). These differences suggest that some EAATs might play physiological roles as substrate-gated anion channels involved in the regulation of cellular excitability, and others may play roles as glutamate transporters (6, 7).

Whereas key processes underlying glutamate transport have been identified in recent years (8–15), molecular determinants of the EAAT anion conductance still need to be clarified. For other transport proteins, studies that focused on the functional consequences of single point mutations greatly improved our understanding of basic mechanisms of operation (16–18). We took a similar approach on EAAT anion channels and focused on a point mutation that was first reported by Vandenberg and co-workers (19). Neutralizing a conserved aspartate between TM2 and TM3 (D112A) abolished the substrate dependence of EAAT1 anion currents, suggesting that aspartate 112 functions as the gate of the EAAT1-associated anion channel.

We focused on the effects of the corresponding mutation on a distinct EAAT isoform. EAAT4 exhibits a prominent anion conductance that can be easily studied by voltage clamp analysis in mammalian cells (5, 7, 20). Furthermore it differs in glutamate transport and voltage-dependent gating of the associated anion channel from other EAAT isoforms (3, 5, 21, 22). We here demonstrate that EAAT4 anion channel gating is modified not only by transport substrates but also by permeant anions. D117A modifies the anion conduction process, the interaction with anions, and gating of EAAT4 anion channels.

EXPERIMENTAL PROCEDURES

Heterologous Expression of WT and Mutant EAAT4 in Mammalian Cells—pcDNA3.1(−) *r*EAAT4 was kindly provided by Dr. J. Rothstein (Johns Hopkins University, Baltimore, MD). The D117A point mutation was introduced using the QuikChange™ method and verified by restriction analysis and DNA sequencing. Transient transfection of tsA201 cells was performed using the $Ca_3(PO_4)_2$ technique as previously described (5). To identify cells with a high probability of expressing recombinant transporters, the cells were cotransfected with a plasmid encoding the CD8 antigen and incubated 5 min before use with polystyrene microbeads precoated with anti-CD8 antibodies (Dynabeads M-450 CD 8; Dynal, Great Neck, NY). The CD8/EAAT4 cDNA ratio and incubation time

* This work was supported by Deutsche Forschungsgemeinschaft Grant Fa301/9-1 (to C. F.).

[S] The on-line version of this article (available at http://www.jbc.org) contains supplemental Table S1 and Figs. S1–S3.

[1] To whom correspondence should be addressed: Institut für Neurophysiologie, Medizinische Hochschule Hannover, Carl-Neuberg-Str. 1, D-30625 Hannover, Germany. Tel.: 49-511-532-2876; Fax: 49-511-532-2776; E-mail: kovermann.peter@mh-hannover.de.

[2] The abbreviations used are: EAAT, excitatory amino acid transporter; TM, transmembrane domain; WT, wild type.

after transfection was adjusted to ensure that almost every cell with beads exhibited currents with the characteristic properties shown in Fig. 1. For WT and D117A EAAT4, two independent recombinants were examined and shown to exhibit indistinguishable functional properties.

Electrophysiology—Standard whole cell patch clamp recordings were performed using an Abimek WPC-100 (Abimek, Göttingen, Germany) amplifier. Borosilicate pipettes were pulled with resistances between 1.0 and 2.5 MΩ. If not otherwise stated, the cells were clamped to 0 mV for at least 2 s between two test sweeps. To reduce voltage errors, more than 80% of the series resistance was compensated by an analog procedure, and cells with current amplitudes of >12 nA were excluded from analysis. The currents were filtered at 5 or 10 kHz and digitized with a sampling rate of 50 kHz using a Digidata 1322A AD/DA converter (Molecular Devices, Sunnyvale, CA). The majority of our experiments were performed with symmetric NO_3^- as permeant anion to minimize alterations of the internal anion concentration during the experiments. Standard external solutions contained 140 mM $NaNO_3$, 4 mM KCl, 2 mM $CaCl_2$, 1 mM $MgCl_2$, 5 mM HEPES, pH 7.4, and the standard internal solutions contained 110 mM $NaNO_3$, 2 mM $MgCl_2$, 5 mM EGTA, 10 mM HEPES, pH 7.4. For all of the experiments, we used external and/or internal agar salt bridges made from a plastic tube filled with 3 M KCl in 1.0% agar to connect the Ag/AgCl electrode. Offset potentials were determined at the end of each experiment, and junction potentials were corrected using the JPCalc software (Dr. P. Barry, University of South Wales, Sydney, Australia).

Current-voltage relationships were constructed from instantaneous current amplitudes (I_{inst}) (determined through extrapolation of mono- or biexponential fits to the start of the voltage step), isochronal current amplitudes (I_{iso}) (determined 2 ms after voltage steps to certain test voltages), or steady-state currents (I_{ss}) (measured after reaching steady-state conditions). Relative open probabilities were calculated from instantaneous tail current amplitudes at +135 or −135 mV after 200-ms steps of variable voltages. The acquired activation curves were fit with Boltzmann functions and normalized to the fitted maximum value at the same cell under saturating L-glutamate concentrations.

Anion permeability sequences for WT EAAT4 and D117A EAAT4 were obtained from measurements with the pipette solution containing 110 mM NaCl, 2 mM $MgCl_2$, 5 mM EGTA, 10 mM HEPES, pH 7.4, in the presence of saturating external L-glutamate (100 μM). Each cell was sequentially perfused with an external solution in which $NaNO_3$ was equimolarly substituted with NaSCN, NaBr, or Na_2SO_4. Reversal potentials were determined from resulting current-voltage relationships, and permeability ratios were calculated from Equation 1.

$$E_{rev} = -\frac{RT}{F}\ln\frac{P_X[X^-]_o + P_{Cl}[Cl^-]_o}{P_{Cl}[Cl^-]_i} \quad \text{(Eq. 1)}$$

Permeability ratios for divalent anions were calculated from Equation 2.

$$E_{rev} = -\frac{RT}{2F}\ln\frac{4P_X[X^{2-}]_o + P_{Cl}[Cl^-]_o}{P_{Cl}[Cl^-]_i} \quad \text{(Eq. 2)}$$

Substrate dependences were tested by sequential perfusion of cells with solutions containing different concentrations of L-glutamate or with solutions in which variable amounts of $NaNO_3$ were equimolarly substituted with choline-NO_3. To study the effects of external anions on EAAT4 anion currents, the cells were sequentially perfused with solutions containing saturating substrate concentrations and different concentrations of NO_3^-. In these experiments, NO_3^- was replaced by equimolar amounts of sodium gluconate.

Noise Analysis—The data were digitized at 50 kHz and filtered with a low pass Butterworth filter with a cut-off frequency of 10 kHz. Power spectrum analysis was performed on the steady-state phase of 1-s-long pulses to different potentials using Clampfit 10.0 (Molecular Devices) and fitted with a double Lorentzian function,

$$S = \frac{S(0)_1}{1 + (f/f_{c_1})^2} + \frac{S(0)_2}{1 + (f/f_{c_2})^2} \quad \text{(Eq. 3)}$$

where S and f denote the spectral density and the frequency, and $S(0)$ and f_c are the amplitude and corner frequency of the corresponding Lorentzian term.

Unitary current amplitudes and absolute open probabilities of WT EAAT4 and D117A EAAT4 were computed with an adaptation of stationary noise analysis (22–24). After subtraction of the background noise (σ_0^2) from the current variance (σ_{ss}^2) this term can be referred to as follows.

$$\frac{\sigma_{ss}^2 - \sigma_0^2}{I_{ss}} = i\cdot(1-p) = i - \frac{I_{ss}}{N} \quad \text{(Eq. 4)}$$

Instantaneous current amplitudes (I_{inst}) are proportional to unitary current amplitudes at the same potential ($\sigma_{ss}^2 - \sigma_0^2$).

$$\frac{\sigma_{ss}^2 - \sigma_0^2}{I_{ss}\cdot I_{inst}} = \frac{i}{I_{inst}} - \frac{I_{ss}}{I_{inst}\cdot N} = \frac{1}{const} - \frac{I_{ss}}{I_{inst}\cdot N} \quad \text{(Eq. 5)}$$

Plotting the ratio of the current variance ($\sigma_{ss}^2 - \sigma_0^2$) and the product of the instantaneous and steady-state current amplitudes ($I_{inst}\cdot I_{ss}$) *versus* the quotient of late current amplitudes by instantaneous current amplitudes ($I_{ss}\cdot I_{inst}^{-1}$) provides a linear relationship. Unitary current amplitudes can be calculated as product of the y axis intercept and the instantaneous current amplitudes ($I_{inst}\cdot const^{-1}$), and the slope of the linear regression (N) gives an approximation of the absolute number of channels (N). We additionally determined unitary current amplitudes from the following,

$$i = \frac{\sigma_{ss}^2 - \sigma_0^2}{I_{ss}} + \frac{I_{ss}}{N} \quad \text{(Eq. 6)}$$

using the slope factor rather than the y axis intercept.

Absolute open probabilities were determined using two approaches. Absolute open probabilities equal ratios of macroscopic current amplitudes (I) by unitary current amplitudes (i) and the number of channels (N) ($p = I/N_i$). Additionally, absolute open probabilities can be calculated from macroscopic current amplitudes and the fitted x axis intercept from noise-current (($\sigma_{ss}^2 - \sigma_0^2)/I_{ss}$ *versus* $I_{ss}\cdot I_{inst}^{-1}$) plots (see Fig. 2, *C* and *D*). Current variances assume zero values when all anion channels

are open, and the absolute open probability is therefore 1. Absolute open probabilities can therefore be calculated from $I_{ss} \cdot I_{inst}^{-1}$ after normalization to the *x* axis intercept.

Kinetic Modeling—Simulations of EAAT4 anion channel open probabilities were performed by solving differential equations on the basis of a modified *r*EAAT2 model (25). Several parameters of the model were estimated by fitting model predictions to experimentally determined activation curves. Fitting was done using a genetic algorithm for minimization of squared errors in the MATLAB environment (The MathWorks).

Homology Modeling—A homology model of the tertiary structure of *r*EAAT4 was built with the SWISS-MODEL Workspace by using the Protein Data Bank entries 2NWX (outward facing conformation, Glt_{Ph}) and 3KBC (inward facing conformation, Glt_{Ph}) as template. The structures were visualized with the ICM Browser Pro (Molsoft LLC) (26).

Data Analysis—The data were analyzed with a combination of pClamp10 (Molecular Devices) and SigmaPlot (Jandel Scientific, San Rafael, CA). For statistical evaluations, Student's *t* test and paired *t* test with $p \leq 0.05$ (*) as the level of significance were used ($p \leq 0.01$ (**), $p \leq 0.001$ (***)). The data are given as the means ± S.E.

RESULTS

D117A Modifies Time and Voltage Dependence of EAAT4 Anion Currents—We expressed WT and D117A EAAT4 heterologously in tsA201 cells and measured ionic currents through the whole cell patch clamp technique (Fig. 1). Internal dialysis with Na^+-based internal solutions and the use of NO_3^- as main internal and external anion resulted in EAAT4 anion currents that are significantly larger than uptake currents and endogenous currents and thus permitted measurements of EAAT4 anion currents in isolation (5).

WT EAAT4 currents rose instantaneously upon voltage steps in the absence of L-glutamate. The instantaneous rise was followed by current activation at negative voltages and by time-dependent decreases of the current amplitudes at positive potentials (Fig. 1*A*). Neutralization of Asp^{117} causes profound changes in the voltage dependence of EAAT4 anion channels (Fig. 1*B*). Depolarizing voltage steps induce voltage-dependent activation of D117A EAAT4 anion currents, whereas current amplitudes are time-independent upon membrane hyperpolarization. Without L-glutamate, depolarization-induced activation is followed by a slow inactivation.

Glutamate has different effects on WT and mutant EAAT4 anion currents. In the presence of glutamate, membrane hyperpolarization induces current deactivation instead of current activation (Fig. 1*A*). The glutamate-induced change in WT EAAT4 anion channel gating results in different glutamate-dependent increases of instantaneous (Fig. 1*C*) and late (Fig. 1*E*) current amplitudes. For D117A EAAT4, glutamate increases instantaneous and late current amplitudes only slightly at positive potentials (Fig. 1, *D* and *F*). At negative voltages, current amplitudes are even decreased by L-glutamate (at −125 mV, $p \leq 0.001$, $n = 20$). L-Glutamate additionally impairs inactivation at positive potentials. We conclude that D117A modifies substrate- and voltage-dependent gating of EAAT4 anion channels.

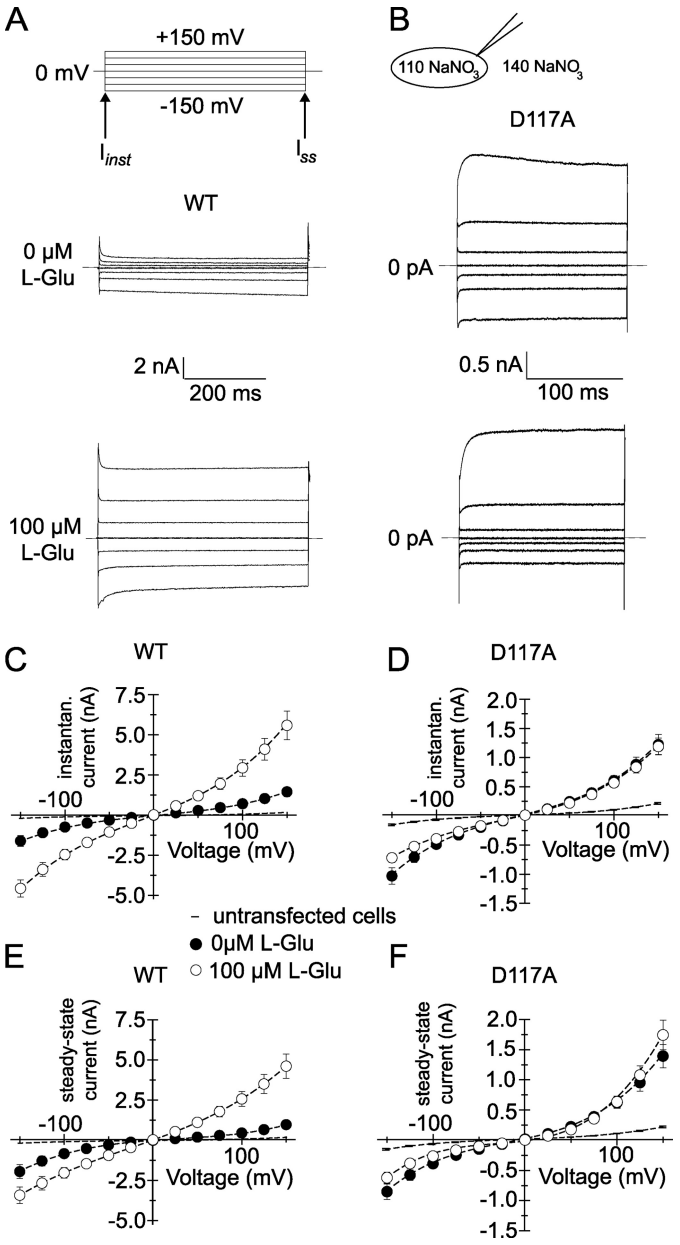

FIGURE 1. **D117A modifies the time and voltage dependence of EAAT4-mediated anion currents.** *A* and *B*, representative current recordings from cells expressing WT EAAT4 (*A*) or D117A EAAT4 (*B*). The experiments were performed in the absence (*top panels*) and in the presence (*bottom panels*) of saturating [L-glutamate] (under standard internal and external solutions). *C* and *E*, current-voltage relationships of the instantaneous (I_{inst}, *C*) and the steady-state current (I_{ss}, *E*) of tsA201 cells expressing WT EAAT4 in the absence (*closed symbols*) and in the presence (*open symbols*, each $n = 5$) of saturating [L-glutamate]. *D* and *F*, current-voltage relationships of the instantaneous current (I_{inst}, *D*) and the steady-state current (I_{ss}, *F*) mediated by D117A EAAT4. Background currents are given as current-voltage relationships of untransfected tsA201 in the presence of saturating [L-glutamate] cells by a simple line with *error bars* ($n = 5$).

Glutamate Increases EAAT4 Anion Currents by Modifying Absolute Open Probabilities—To study the effects of D117A at the level of individual proteins, we performed noise analyses on WT and mutant EAAT4 (Fig. 2). We first determined power spectra from macroscopic anion currents using fast Fourier

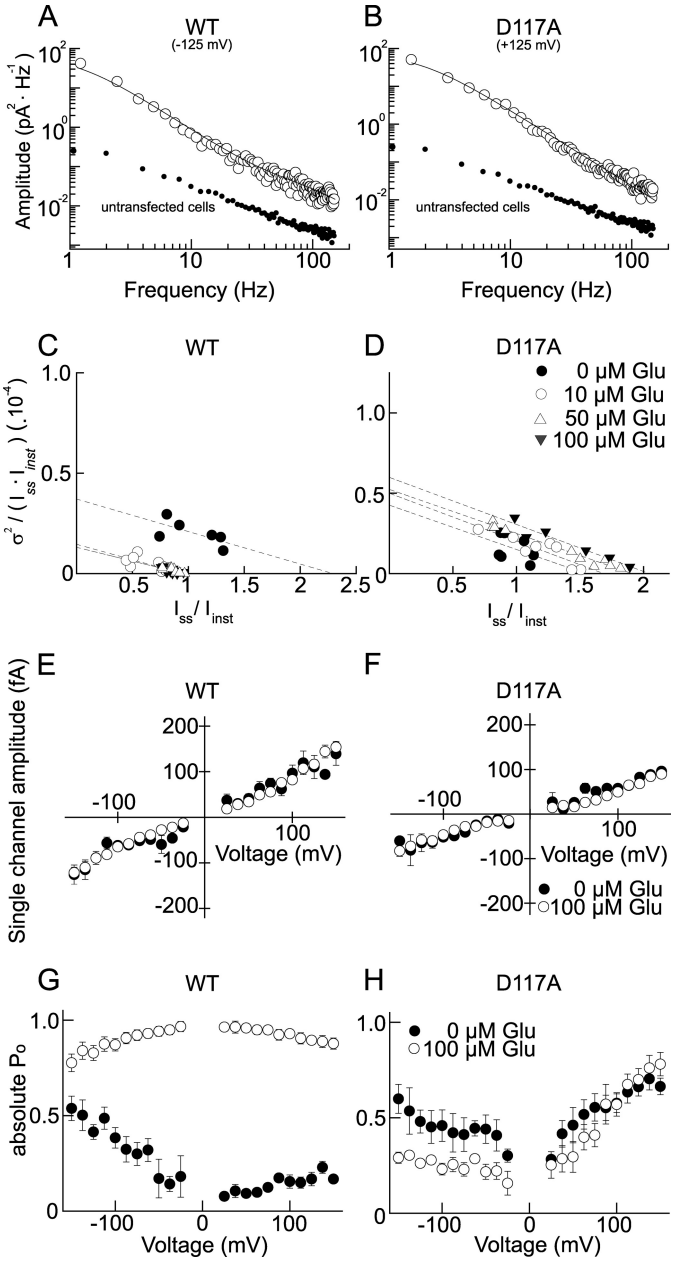

FIGURE 2. **D117A modifies unitary conductance and absolute open probability of EAAT4 anion channels.** *A* and *B*, power density spectra of WT (*A*) and D117A EAAT4 (*B*) from current recordings at −125 mV (WT) and +125 mV (D117A) with 100 μM L-glutamate. Fits with double Lorentzian functions are given as *solid lines*, and background power density spectra of untransfected tsA201 cells are given as *filled circles*. *C* and *D*, representative stationary noise analyses for WT EAAT4 (*C*) and D117A EAAT4 (*D*). *E* and *F*, voltage dependence of unitary anion currents of WT (*E*) and D117A EAAT4 (*F*) derived from stationary noise analysis (n = 9/9). *G* and *H*, absolute open probabilities for WT (*G*) and D117A EAAT4 (*H*). The *open symbols* give values determined in the presence of 100 μM glutamate, and the *filled symbols* give values determined in its absence.

transformation (27). For WT as well as for D117A EAAT4, the acquired power spectra can be well fit with a sum of two Lorentzian components. Corner frequencies f_c are predicted to reflect macroscopic current relaxation time constants τ_m by the relation $f_c = 1/(2\pi\tau_m)$. The acquired corner frequencies for WT (at −125 mV: 1.2 Hz and 103.9 Hz) and D117A (at +125 mV: 1.8 Hz and 16.8 Hz) were in accordance with the relaxation time constants of EAAT4 anion currents (WT, τ_1 = 2.6 ± 0.7 ms; τ_2 = 36.4 ± 3.6 ms, n = 8; D117A: τ = 10.5 ± 1.1 ms, n = 16). Untransfected tsA201 cells showed lower current variances and power spectra resembling 1/f noise under the same conditions (Fig. 2, *A* and *B*). These results demonstrate that, for WT and mutant EAAT4, anion current-associated noise arises from the random opening and closing of individual channels and can be used to determine amplitudes of the underlying single channel opening.

We employed a variation of stationary noise analysis (22–24, 28). Steady-state current variances (σ^2) and mean current amplitudes (I_{ss}) were measured at various voltages and glutamate concentrations. The variances were divided by the corresponding steady-state and instantaneous current amplitudes determined at the same potential and [L-glutamate]. The acquired ratios were then plotted *versus* the ratio of mean and instantaneous current amplitudes (Fig. 2, *C* and *D*). This transformation enables a calculation of the unitary pore properties by a linear fit to the values obtained from measurements of the current variances. The slope ($-N^{-1}$) of the fitted straight gives the number of channels N, and the y axis intercept provides the scaling factor ($const^{-1}$), representing the ratio of unitary current and instantaneous current amplitudes. Linear fits provided mean regression coefficients (r^2) of 0.71 for EAAT4 WT and 0.84 for EAAT4 D117A, indicating strong linear correlation between the data points. The relative errors of the slope factors were on average ± 17% for WT and ± 18% for D117A EAAT4, respectively.

Multiplication of the thus acquired scaling factors with instantaneous current amplitudes provided the voltage dependence of unitary current amplitudes of WT and D117A EAAT4 anion channels at various external glutamate concentrations (Fig. 2, *E* and *F*). For WT and mutant EAAT4, application of glutamate modified neither the number of transporters nor the unitary conductance. D117A decreases single channel amplitudes of EAAT4 anion channels by ~40% (WT EAAT4: 123.2 ± 11.5 fA and D117A EAAT4: 73.3 ± 7.0 fA, at +125 mV, n = 8/9). We compared these data with unitary conductances calculated according to Equation 6 (WT EAAT4: 116.4 ± 10.5 fA and D117A EAAT4: 74.5 ± 9.2 fA, at +125 mV, n = 9/9). Both calculations revealed similar results for WT and D117A EAAT4.

Absolute open probabilities were calculated using two approaches, *i.e.* from the number of transporters (N) and the unitary conductance (i) ($p = I/N_i$) (Fig. 2, *G* and *H*), as well as from I_{ss}/I_{inst} after normalization to the x axis intercept in Fig. 2 (*C* and *D*; and data not shown). Both calculations provided indistinguishable results. In the absence of L-glutamate, WT EAAT4 assumed minimum open probabilities at 0 mV and channel activation upon membrane hyperpolarization. Saturating glutamate concentrations increased absolute open probabilities and altered their voltage dependence. At 100 μM L-glutamate, the voltage dependence of the absolute open probability of WT EAAT4 is a bell-shaped function with its maximum at ~0 mV (Fig. 2*G*). Before application of glutamate, the open probability of D117A EAAT4 was at a minimum at ~0 mV and increased upon membrane depolarization or hyperpolarization. 100 μM L-glutamate decreased the D117A steady-

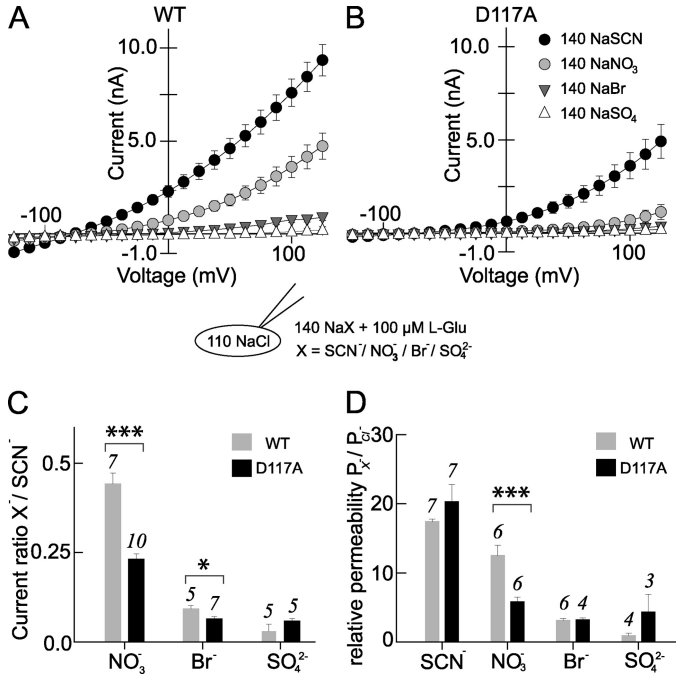

FIGURE 3. **D117A modifies relative anion permeabilities of EAAT4 anion channels.** *A* and *B*, current-voltage relationships for WT (*A*) and D117A EAAT4 (*B*) at four different external anions (140 mM SCN^-, NO_3^-, Br^-, SO_4^{2-}) in the presence of 100 μM L-glutamate. The cells were dialyzed with Cl^--based internal solution. *C* and *D*, relative current amplitudes at +125 mV (*C*) and permeabilities (*D*) for WT and D117A EAAT4.

state absolute open probabilities at negative voltages and rendered them almost unaltered at positive voltages (Fig. 2*H*).

Anion Selectivity of WT and Mutant Channels—To test whether D117A also affects the selectivity of EAAT4 anion channels among different anions, WT and D117A EAAT4 anion currents were studied at asymmetric anion conditions. The cells were held at −80 mV, dialyzed with a Cl^--based solution, and sequentially perfused with different external solutions. Fig. 3 (*A* and *B*) shows current-voltage relationships for WT and D117A EAAT4 for various external anions. D117A altered relative conductivities for Br^- and NO_3^- (Fig. 3*C*). Another parameter that can be used to quantify alterations of anion selectivity is the relative permeability ratio (29). We calculated permeability ratios for WT and D117A EAAT4 from reversal potentials under various external solutions using the Goldman-Hodgkin-Katz equation. D117A significantly changed the P_{NO_3}/P_{Cl} permeability ratio ($p \leq 0.001$, $n = 7$) but left other ratios unaffected (Fig. 3*D*).

Distinct Gating Processes in WT and Mutant EAAT4 Anion Channels—WT as well as D117A EAAT4 exhibit biphasic gating (Fig. 1) that likely arises from the existence of two gating processes with different voltage dependence. In the following we will refer to one specific process that is activated by depolarization as activation and to the other process with inverse voltage-dependent gating as inactivation.

We took advantage of the different time courses to separate the voltage dependences of these two gating processes. Supplemental Fig. S1*A* illustrates the separation procedure for WT EAAT4 at 100 μM L-glutamate. Open probabilities were determined by plotting instantaneous current amplitudes at a fixed test step to −135 mV *versus* the preceding voltage. The acquired voltage dependence of relative open probabilities resembles the voltage dependence of absolute open probabilities obtained by noise analysis (Fig. 2*G*). After depolarizing prepulses, steps to −135 mV result in initial current increases on a fast time course to certain maximum amplitudes and consecutive deactivation. The initial increase is due to recovery from inactivation that has occurred during the preceding pulse. Extrapolating current amplitudes to the beginning of the inserted voltage steps using a monoexponential function allows determination of the voltage dependence of the relative open probabilities of the activation gate (supplemental Fig. S1, *A* and *C*, *red circles*). Assuming that activation and inactivation are independent, relative open probabilities of the inactivation gate (*green squares*) were then calculated by dividing the channel activation curve (*blue circles*) by the relative open probabilities of the activation gate (supplemental Fig. S1*E*, *red circles*).

A comparable separation of gating processes in D117A EAAT4 revealed depolarization-induced activation and subsequent inactivation, however, with different voltage dependences (supplemental Fig. S1, *B*, *D*, and *F*). We plotted instantaneous current amplitudes at +135 mV *versus* the preceding potential to obtain the voltage dependence of the open probability (supplemental Fig. S1, *B* and *D*). Steps to +135 mV cause activation of D117A EAAT4 anion channels, and the maximum amplitude at this potential thus solely depends on the number of channels that were not inactivated at the end of the prepulse. Assuming that activation and inactivation occur independently of each other, we divided open probabilities of channels by the acquired inactivation curve to obtain the separated activation curve (supplemental Fig. S1*F*). This analysis reveals a significant shift of the activation curve by D117A. Because inactivation of D117A is very slow, we were unable to perform this analysis under conditions that allow determination of steady-state inactivation curves.

Glutamate-dependent Changes in Voltage-dependent Gating—We next determined open probabilities of WT and D117A EAAT4 anion channels for various L-glutamate concentrations. Because unitary current amplitudes are unaffected by the external substrate concentration (Fig. 2, *E* and *F*), relative open probabilities were calculated from instantaneous tail current amplitudes after normalization to values obtained at saturating glutamate concentrations. Whereas absolute open probabilities of WT EAAT4 change significantly with [glutamate], there are only minor effects of the external glutamate concentration on mutant channels (Fig. 4, *A* and *B*).

Fig. 4 (*C*–*F*) shows separated activation (Fig. 4, *C* and *D*) and inactivation (Fig. 4, *E* and *F*) curves for various glutamate concentrations. For WT EAAT4, activation curves were similar at 0 and 10 μM L-glutamate. At higher concentrations, there is a substrate-dependent saturable shift of the activation curve to more positive voltages (Fig. 4*C*). The voltage dependence of steady-state activation did not reach the inflection point, precluding accurate fits with Boltzmann functions for all tested glutamate concentrations. There is an additional glutamate-dependent shift of the inactivation curve to more positive voltages (Fig. 4*E*), resulting in a significantly decreased number of open channels at voltages positive to −100 mV.

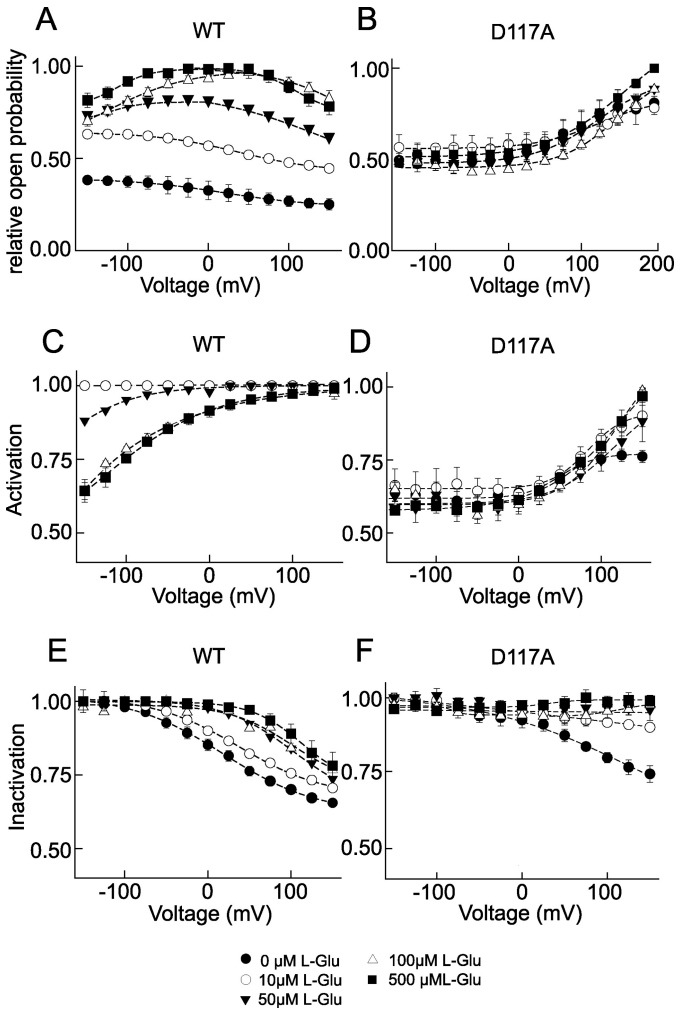

FIGURE 4. **Modulation of EAAT4 anion channel gating by L-glutamate.** *A* and *B*, voltage dependence of relative open probabilities at various [L-glutamate] for WT (*A*) and D117A EAAT4 (*B*). *C* and *D*, voltage dependence of relative open probabilities of the activation gate of WT (*C*) and D117A EAAT4 (*D*). *E* and *F*, voltage dependence of relative open probabilities of the inactivation gate of WT (*E*) and D117A EAAT4 (*F*).

For D117A EAAT4, the activation curve is only slightly affected by external [L-glutamate] (Fig. 4*D*). However, glutamate removes inactivation in a concentration-dependent manner (Fig. 4*F*).

Sodium Dependence of WT and Mutant EAAT4 Anion Channels—Activity of EAAT anion channels critically depends on external [Na^+] (Fig. 5) (20, 30, 31). Removal of Na^+ dramatically decreases WT and mutant anion currents (Fig. 5, *A* and *D*). However, the relative sodium-dependent steady-state current amplitudes as well as the concentration dependence of anion currents were different for WT and D117A EAAT4 (Fig. 5).

In the absence of glutamate at −125 mV, the sodium dependence of WT EAAT4 can be described with a Hill function with an apparent K_D of 64.8 ± 6.6 mM and a Hill coefficient of 2.1 ± 0.3 ($n = 4$; Fig. 5*B*). At +125 mV, the K_D was significantly larger, precluding accurate determination under our conditions (Fig. 5*B*). Saturating [L-glutamate] (5 mM) decreased the apparent K_D values at positive (at +125 mV: $K_D = 10.9 \pm 0.5$ mM, $n_H = 1.5 \pm 0.1$ ($n = 5$)) as well as at negative potentials (at −120 mV: $K_D = 3.9 \pm 0.3$ mM, $n_H = 2.6 \pm 0.1$ mM, $n = 5$) (Fig. 5*C*). D117A changes apparent dissociation constants, Hill coefficients, and the voltage dependence of the anion current modification by Na^+ (Fig. 5*D*). At negative voltages D117A EAAT4 was only slightly activated by sodium in the absence of L-glutamate (Fig. 5, *D* and *E*). At +125 mV, Na^+ increases D117A EAAT4 anion currents with a $K_D = 13.1 \pm 0.8$ mM and $n_H = 1.5 \pm 0.3$ ($n = 7$) (Fig. 5*E*). At [L-glutamate] = 5 mM, D117A EAAT4 anion currents were decreased at negative potentials and increased at positive voltages ($K_D = 7.0 \pm 0.9$ mM, $n_H = 1.2 \pm 0.2$ ($n = 4$)) (Fig. 5, *D* and *F*).

Anion Dependence of WT and Mutant EAAT4 Anion Channels—The alteration of the unitary conductance of EAAT4 anion channels (Fig. 2*F*) suggested that D117A might affect gating via altered anion dependence (5). We therefore studied WT and mutant EAAT4 anion channel gating at different external [NO_3^-] in the presence of saturating [glutamate] (Fig. 6).

At an external nitrate concentration of 1 mM, WT anion current deactivation at negative voltages is much more pronounced than under standard conditions (Fig. 6*A*). In contrast, varying external [NO_3^-] did not change the time and voltage dependence of D117A anion currents (Fig. 6*B*). To study the role of permeant anions in modifying anion channel gating, we determined relative open probabilities as well as activation and deactivation time constants in the presence of different external [NO_3^-] (Fig. 6). In WT EAAT4, activation curves are shifted to more positive potentials with decreasing [NO_3^-] (Fig. 6*C*). Deactivation time constants are increased in a concentration-dependent manner (Fig. 6*E*). These results indicate that NO_3^- prevents closure of the activation gate. No anion dependence of WT channel inactivation could be observed (data not shown).

D117A abolishes anion-dependent gating of EAAT4 anion channels. Neither activation time constants nor voltage dependence of activation of D117A EAAT4 was modified when [NO_3^-] was changed between 10 and 140 mM (Fig. 6, *D* and *F*). With external glutamate, D117A EAAT4 did not inactivate at any tested [NO_3^-].

Gating of EAAT4 Anion Channels Is Not Exclusively Determined by Transitions within the Glutamate Uptake Cycle—All kinetic models of glutamate transporters published so far are based on a tight coupling between transitions in the glutamate uptake cycle and opening and closing of the anion channel. In these models, distinct open probabilities are attributed to certain states of the transport process (21, 25, 31). Modification of the anion channel function might be caused either by altered distribution of the transporter within the uptake cycle or by changes of anion channel open probabilities assigned to the different states.

We studied whether gating of WT and D117A EAAT4 anion channel gating can be described by a modification of the most complete existing kinetic model that was developed for EAAT2 (25) (Fig. 7*A*). Because glutamate uptake by EAAT4 is thought to occur by the same molecular mechanism and stoichiometry as in EAAT2 (21) and because our analysis is based on steady-state conditions, we decided to use the same uptake cycle rate constants as for EAAT2 (25). To account for EAAT4-specific channel gating, we attributed open probability values (p_1 to p_7)

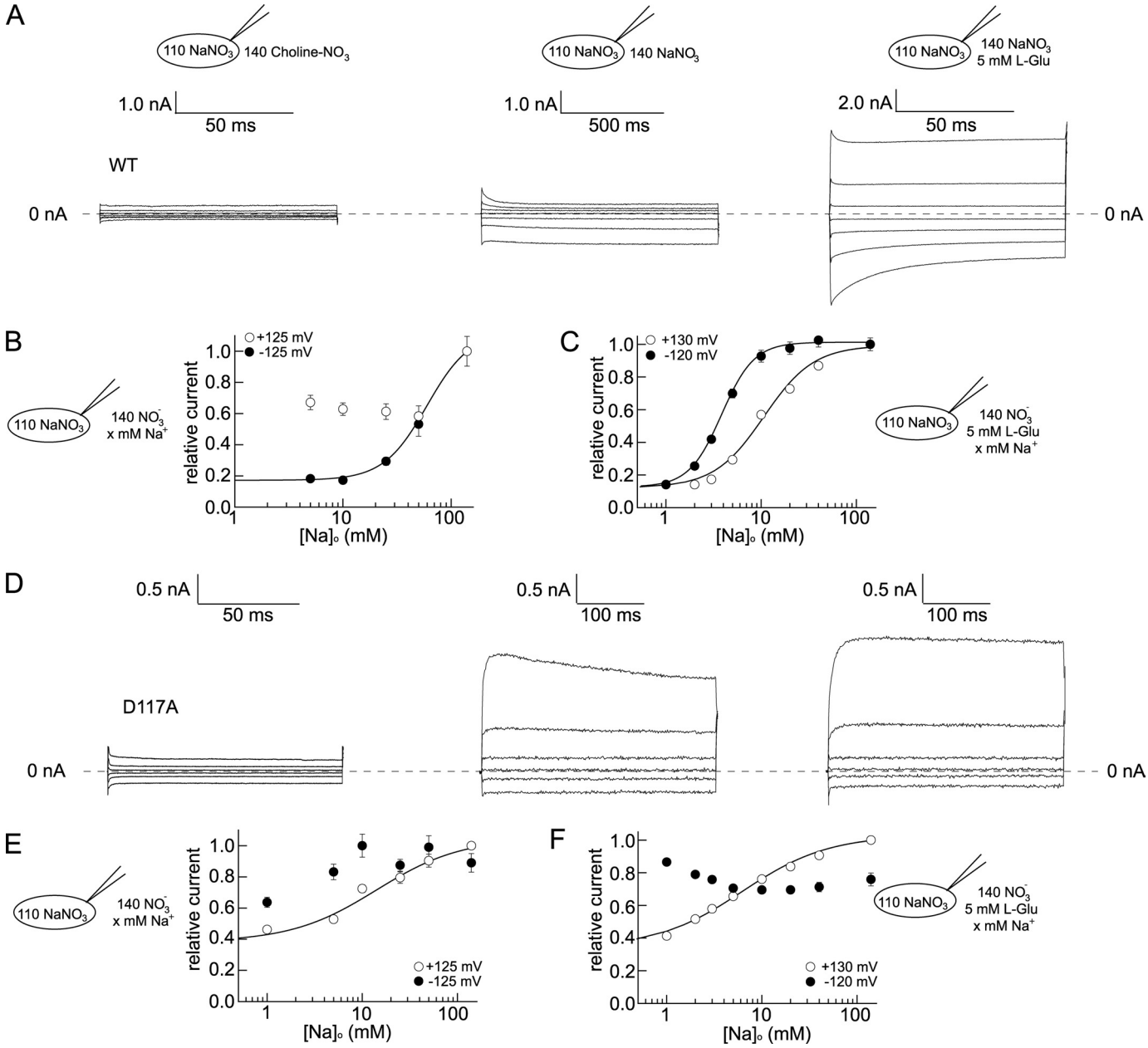

FIGURE 5. **Sodium dependences of WT and mutant EAAT4.** *A* and *D*, representative current recordings of WT (*A*) and D117A (*D*) EAAT4 in the absence of L-glutamate and sodium (*left panel*), in the presence of sodium (*middle panel*), and in the presence of sodium and L-glutamate (*right panel*). *B*, *C*, *E*, and *F*, sodium dependence of late WT (*B* and *C*) and D117A EAAT4 anion currents (*E* and *F*), in the absence (*B* and *E*), or in the presence of external glutamate (*C* and *F*).

to several states of the transport cycle (24). These parameters were estimated for WT and D117A by fitting simulated open probabilities to experimentally determined absolute open probabilities at various voltages and [L-glutamate] (supplemental Table S1).

Initially, we assumed independence of the transport cycle and the channel state (referred to as model 1; Fig. 7*A*) and thus assigned open and closed channel state to various states of the transport cycle. For WT EAAT4 this approach did not succeed in defining parameters that correctly predict the experimentally determined absolute open probabilities and their voltage dependence. The model was only able to mimic certain aspects of EAAT4 gating when measured open probabilities were scaled down at least 5-fold for the fitting process. However, the model was able to reproduce the main features of D117A gating, such as the shift of the voltage dependence of the open probability to the right, absolute open probabilities, and the glutamate dependence of the mutant transporters (Figs. 2*H* and 7*B*). We conclude from this simulation that WT EAAT4 anion channel gating is only partially determined by transitions within the uptake cycle.

Because the external anion concentration modifies gating of WT EAAT4 (Fig. 6), we extended model 1 by adding open states branching from the transport cycle (model 2; Fig. 7*C*). In this scheme, the uptake cycle cannot proceed as long the channel is open, resulting in a switch between transport and anion conduction mode. Such a modification gave almost perfect predictions for absolute open probabilities in the presence and

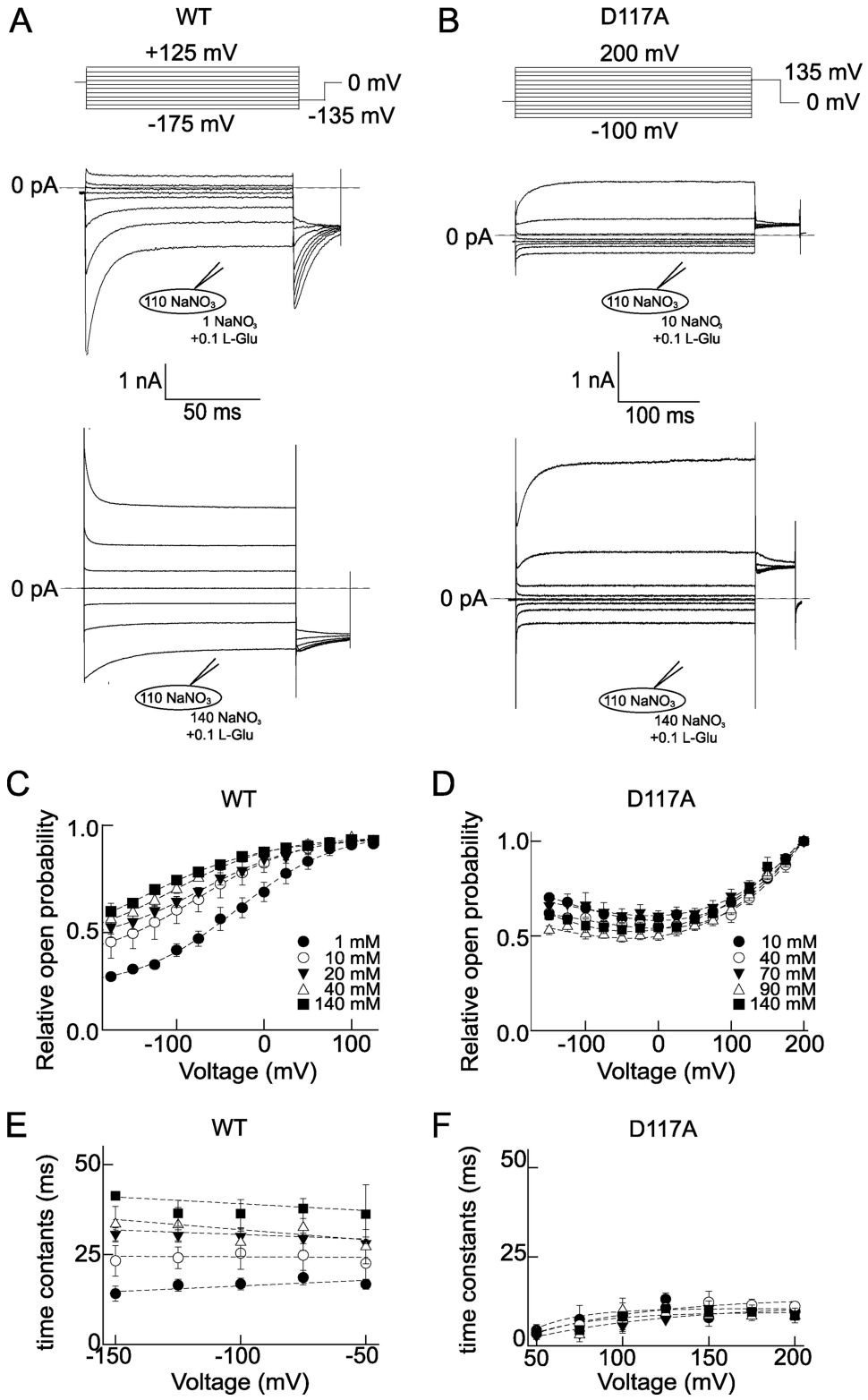

FIGURE 6. **Anion dependence of WT and D117A EAAT4 anion channel gating.** *A* and *B*, representative current recordings for varying external [NO_3^-] from cells expressing WT (*A*) and D117A EAAT4 (*B*). *C* and *D*, separated activation curves from WT EAAT4 (*C*) and D117A EAAT4 (*D*) under different external anion conditions. *E* and *F*, voltage dependences of the time constants (τ) of activation/deactivation for WT (*E*) and D117A EAAT4 (*F*).

absence of glutamate in both WT and D117A except for some deviations in the glutamate dependence at negative voltages, which might be due to differences in the substrate affinities in EAAT2 and EAAT4 (Fig. 7*D*). Furthermore, model 2 relates the glutamate-induced reduction of channel open probability at negative potentials in D117A EAAT4 and the altered response to sodium application to the simple assumption of changed open probability values (p_1 to p_7) in the D117A mutant (supplemental Fig. S2).

DISCUSSION

EAATs function as coupled transporters and also as anion channels. Differences in anion selectivity among distinct EAAT isoforms (5), mutagenesis studies (19, 32), and reconstitution experiments with purified bacterial homologs (33) demonstrated that the anion conduction pathway is formed by the EAAT protein itself. Bi-ionic reversal potentials depend on the absolute concentration of anions, indicating that anion permeation occurs through a multi-ion aqueous conduction pathway (5) and not by alternating access-type transport processes.

So far, the anion-selective pore of EAAT anion channels has not been identified. Moreover, the basic features of EAAT4 anion channels have been unclear for many years. In a recent review, Vandenberg *et al.* (34) distinguished two types of EAAT-associated anion conductances. The so-called anion leak conductance is active in the absence of glutamate and depends on the extracellular [Na^+]. Application of glutamate induces a substrate-activated anion conductance that differs from the leak current in relative anion permeabilities (5, 19, 32). Two alternative explanations for these functional alterations were discussed (34), a single ion conduction pathway that is functionally modified by substrates and a separate substrate-dependent conduction pathway. Our results strongly support the first possibility. Glutamate modifies neither the unitary conductance nor the number of active anion channels (Fig. 2). Moreover, leak and substrate-dependent conductances exhibit closely similar voltage-dependent gating (Fig. 1). Our finding that glutamate does not affect uni-

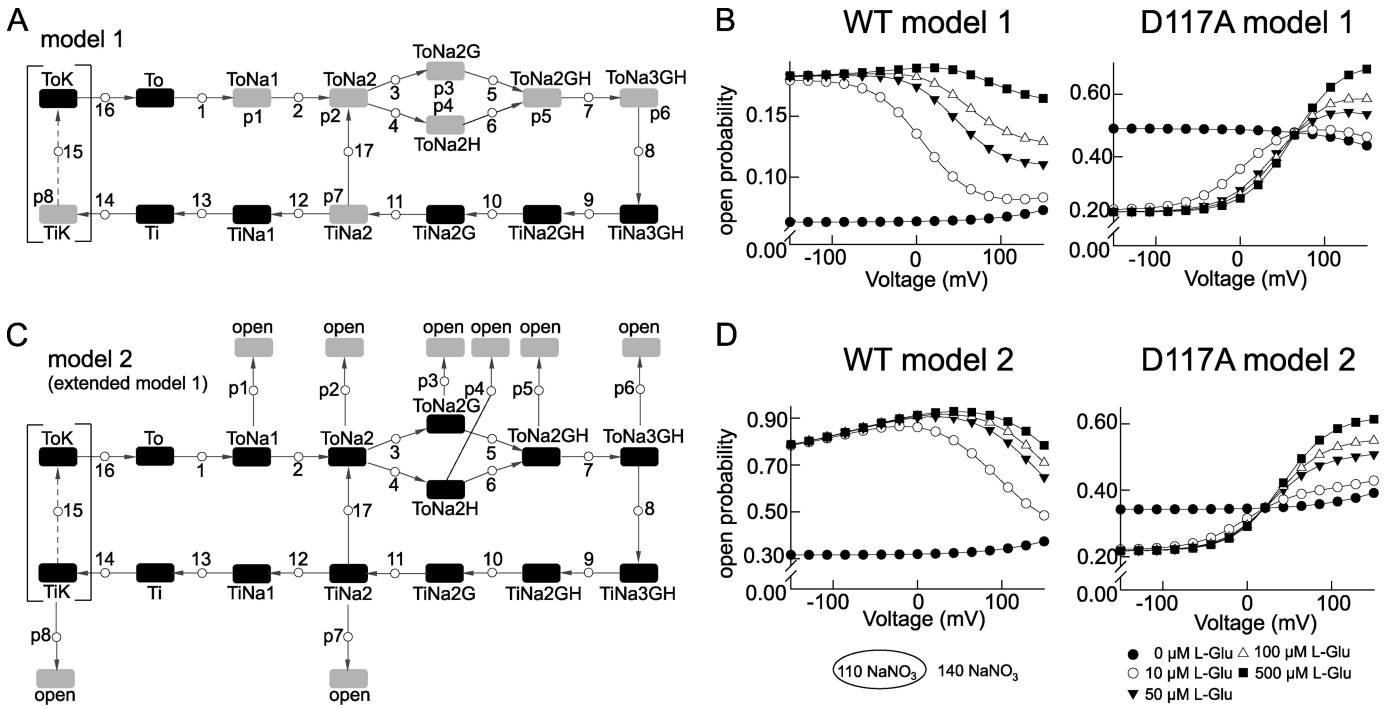

FIGURE 7. **Kinetic model of the EAAT4 transporter.** *A*, state diagram of the stoichiometrically coupled glutamate transport cycle (model 1) based on a published *r*EAAT2 model (29). The transport process is assumed to be unaltered by the channel being open or closed. *B*, simulated WT and D117A EAAT4 activation curves using model 1. *C*, modified state diagram that assumes explicit switching between anion conduction and transport mode (model 2). *D*, simulated WT and D117A EAAT4 activation curves using model 2 shown in *C*.

tary current amplitudes shows evidence contrary to the recent proposal that distinct states of the glutamate transport cycle assume anion conducting states with different unitary conductances (12).

In the absence of glutamate, WT and D117A EAAT4 anion channels exhibit comparable absolute open probabilities (Fig. 2). However, whereas glutamate increases WT EAAT4 anion currents up to 4-fold, D117A EAAT4 anion currents are only slightly augmented at positive potentials and even decreased at negative voltages. In contrast to the virtual glutamate independence of D117A EAAT4, mutant channels were activated by increasing external $[Na^+]$ to a similar extent as WT. D117A therefore does not affect anion current amplitudes by disabling the anion channel gate as proposed for D112A EAAT1 (19) but rather by modifying its opening and closing processes. In agreement with this notion, D117A results in pronounced changes in the voltage dependence of EAAT4 anion channel gating (Fig. 1).

D117A modifies various pore properties of EAAT4 anion channels. Noise analysis reveals decreased unitary current amplitudes by ~40% without changes in rectification. D117A is thus the first reported mutation that modifies unitary conductances of the EAAT anion channel. In agreement with alteration of pore properties, D117A EAAT4 anion channels exhibit altered relative anion permeabilities. Relative permeabilities and conductivities were decreased for NO_3^-. Taken together, these results indicate that Asp^{117} is in close spatial proximity to the anion conduction pathway. However, the finding that neutralizing a negative side chain decreases anion transport rates suggests that permeating ions are not in contact with the Asp^{117} side chain.

Single channel amplitudes of WT and mutant EAAT4 are below the resolution limit of single channel recordings and can therefore only be studied by noise analysis. We used a modification of stationary noise analysis that utilizes linear fits and extrapolation to the *y* axis intercepts (22, 24) (Fig. 2, *C* and *D*). Under certain conditions this approach requires extrapolation over substantial relative current intervals. In this case extrapolation might cause significant errors in *y* axis intercepts even for moderate errors in slope factors. Several lines of evidence support the notion that we accurately determined unitary conductances and absolute open probabilities. Standard errors of unitary current amplitudes are quite small. Moreover, unitary current amplitudes determined by data extrapolation resemble amplitudes determined using another mathematical approach. Lastly, absolute open probabilities were determined with two different approaches, and both approaches resulted in comparable values.

D117A causes pronounced alterations of voltage-dependent gating (Fig. 1). To describe these alterations in detail, WT and mutant EAAT4 anion channel gating was analyzed under a variety of conditions. WT anion channels exhibit two different gating processes with inverse voltage dependence. Separation of these two processes (supplemental Fig. S1) demonstrated that one of these processes, depolarization-induced activation, is affected by glutamate and by the external anions. Glutamate shifts the activation curve to more positive potentials (Fig. 4), whereas external anions modify EAAT4 activation in a way reminiscent of the "foot-in-the-door" phenomenon of potassium channels (35). High external $[NO_3^-]$ increases the probability of the channel to be open and slows channel deactivation

(Fig. 6, *C* and *E*). These findings demonstrate not only that the EAAT4 anion channel is a substrate-gated channel with a tight coupling of channel opening and closing to conformational changes of the corresponding carrier domain but that opening and closing are also modified by occupation of the anion channel pore.

Depolarizing voltage steps not only activate WT EAAT4 anion channels but promote another gating process that we refer to as channel inactivation. Glutamate also modifies the voltage dependence of WT inactivation by shifting the voltage dependence of inactivation to more positive potentials (Fig. 4). In contrast to EAAT4 anion channel activation, inactivation is not affected by external anions.

D117A abolishes glutamate and anion modulation of channel activation. Moreover, it shifts the voltage dependence of channel activation to more positive voltages (Fig. 4). In contrast, EAAT4 anion channel inactivation is only slightly altered by this point mutation (Fig. 4).

D117A modifies the sodium dependence of EAAT4 anion currents in the absence as well as in the presence of glutamate (Fig. 5). Increased [Na^+] reduced D117A EAAT4 currents at negative potentials but augmented current amplitudes at positive voltages. In contrast, Na^+ activates WT EAAT4 anion channels over the whole voltage range (Fig. 5) (25, 36). Because glutamate-associated changes of anion currents are too insignificant to be accurately determined, we were unable to quantify binding of glutamate to D117A EAAT4.

There are several possible explanations for the joint effects of D117A on anion conduction and on the substrate dependence of anion currents. Asp^{117} could be in close proximity to the anion conduction pathway as well as to the sodium-binding sites. At present, high resolution structures exist for the archeal transporter Glt_{Ph} in two conformations, one with substrate-binding sites accessible to the external medium, in the outward facing conformation (9), and another one in the inward facing conformation (11). Comparison of the two conformations lead to the definition of a "trimerization domain" (containing TM1, TM2, TM4, and TM5) that is largely immobile and a "translocation domain" undergoing substantial movements during the glutamate transport process (11). The loop between TM2 and TM3 marks the border between the two domains. During the transitions between the outward and inward facing conformations, TM3 is shifted relative to TM2, resulting in an altered orientation of TM2–TM3 loop. Asp^{117} is not conserved in Glt_{Ph} (supplemental Fig. S3*A*). However, homology models of EAAT4 to Glt_{Ph} structures predict a rotational movement of Asp^{117}, as part of the TM2-TM3 loop, upon transition from the outward to the inward-facing conformation (supplemental Fig. S3*B*). One might speculate that D117A primarily affects this transition and that changes in the uptake cycle are the basis of the observed alterations in anion channel gating. Two lines of evidence argue against such an explanation. In EAAT1, D112A resulted only in minor alterations of glutamate uptake (19). Moreover, D117A-induced alterations of EAAT4 anion channel gating cannot be simulated by varying the rate constants for the glutamate translocation connecting inward and outward facing conformation (data not shown).

The distance between Na^+ ions and Asp^{117} is between 16 Å in the inward and 24 Å in the outward facing conformation (supplemental Fig. S3*B*). This distance makes a direct effect on Na^+ binding unlikely. This notion is further supported by the finding that D117A modifies Na^+ binding in the absence and in the presence of glutamate (Fig. 5) and that neutralization of negatively charged residue cannot increase the affinity of Na^+-binding sites by direct electrostatic interaction. Finally, Asp^{117} is conserved in *Escherichia coli* glutamate transporter, which functions independently of Na^+ (37).

Alternatively, D117A might cause global conformational changes that affect secondary active transport and channel function. The structural conservation of prokaryotic and eukaryotic transporters together with the lack of an acidic residue in Glt_{Ph} at this position (9) argues against this possibility.

WT EAAT4 anion channel gating is only predicted by a kinetic model in which anion channel opening locks the uptake cycle in its current state (Fig. 7, *C* and *D*). In contrast, D117A EAAT4 gating is well described by conventional models (Fig. 7, *A* and *B*). We therefore postulate that D117A affects transitions between transporter and channel function of EAAT4. These changes modify EAAT4 anion channel gating and result in altered apparent sodium dependence without a direct effect on Na^+-binding sites (supplemental Fig. S2).

Because permeant anions modify WT but not D117A EAAT4 anion channel gating (Fig. 6), it is tempting to speculate that binding of permeant anions might be necessary for this transition in WT but not in mutant EAAT4. Transitions between the two functional modes of EAATs have not been experimentally demonstrated so far. Such a scenario, however, predicts the existence of transporters with high transport rates and low relative anion currents and others with low transport rates and large relative anion currents (21, 22). Moreover, it explains how external NO_3^- can reduce proton transport rates of glutamate transporter in salamander retina glial cells (38) without being cotransported (2).

In summary, we have studied the role of a pore-forming residue for the function of EAAT4 anion channels. Our data suggest an important role of anions in determining opening and closing of EAAT anion channels. A neutralizing mutation in a conserved aspartate (D117A) affects anion permeation and binding and, via modifying its anion dependence, the opening and closing transitions of EAAT anion channels.

Acknowledgments—We thank Dr. J. Rothstein for providing the expression construct for rEAAT4; Drs. Alexi Alekov, Delany Torres-Salazar, Doreen Nothmann, Gabriel Stölting, Ariane Leinenweber, and Martin Fischer for helpful discussions; and Birgit Begemann and Toni Becher for excellent technical assistance.

REFERENCES

1. Fairman, W. A., and Amara, S. G. (1999) *Am. J. Physiol.* **277,** F481–F486
2. Wadiche, J. I., Amara, S. G., and Kavanaugh, M. P. (1995) *Neuron* **15,** 721–728
3. Fairman, W. A., Vandenberg, R. J., Arriza, J. L., Kavanaugh, M. P., and Amara, S. G. (1995) *Nature* **375,** 599–603
4. Watzke, N., and Grewer, C. (2001) *FEBS Lett.* **503,** 121–125
5. Melzer, N., Biela, A., and Fahlke, Ch. (2003) *J. Biol. Chem.* **278,**

50112–50119
6. Amara, S. G., and Fontana, A. C. (2002) *Neurochem. Int.* **41,** 313–318
7. Melzer, N., Torres-Salazar, D., and Fahlke, Ch. (2005) *Proc. Natl. Acad. Sci. U.S.A.* **102,** 19214–19218
8. Gouaux, E., and Mackinnon, R. (2005) *Science* **310,** 1461–1465
9. Yernool, D., Boudker, O., Jin, Y., and Gouaux, E. (2004) *Nature* **431,** 811–818
10. Boudker, O., Ryan, R. M., Yernool, D., Shimamoto, K., and Gouaux, E. (2007) *Nature* **445,** 387–393
11. Reyes, N., Ginter, C., and Boudker, O. (2009) *Nature* **462,** 880–885
12. Tao, Z., and Grewer, C. (2007) *J. Gen. Physiol.* **129,** 331–344
13. Tao, Z., Zhang, Z., and Grewer, C. (2006) *J. Biol. Chem.* **281,** 10263–10272
14. Larsson, H. P., Tzingounis, A. V., Koch, H. P., and Kavanaugh, M. P. (2004) *Proc. Natl. Acad. Sci. U.S.A.* **101,** 3951–3956
15. Koch, H. P., and Larsson, H. P. (2005) *J. Neurosci.* **25,** 1730–1736
16. Yang, N., and Horn, R. (1995) *Neuron* **15,** 213–218
17. Schoppa, N. E., McCormack, K., Tanouye, M. A., and Sigworth, F. J. (1992) *Science* **255,** 1712–1715
18. Fahlke, Ch., Beck, C. L., and George, A. L., Jr. (1997) *Proc. Natl. Acad. Sci. U.S.A.* **94,** 2729–2734
19. Ryan, R. M., Mitrovic, A. D., and Vandenberg, R. J. (2004) *J. Biol. Chem.* **279,** 20742–20751
20. Torres-Salazar, D., and Fahlke, Ch. (2006) *J. Neurosci.* **26,** 7513–7522
21. Mim, C., Balani, P., Rauen, T., and Grewer, C. (2005) *J. Gen. Physiol.* **126,** 571–589
22. Torres-Salazar, D., and Fahlke, Ch. (2007) *J. Biol. Chem.* **282,** 34719–34726
23. Sigworth, F. J., and Zhou, J. (1992) *Methods Enzymol.* **207,** 746–762
24. Sesti, F., and Goldstein, S. A. (1998) *J. Gen. Physiol.* **112,** 651–663
25. Bergles, D. E., Tzingounis, A. V., and Jahr, C. E. (2002) *J. Neurosci.* **22,** 10153–10162
26. Arnold, K., Bordoli, L., Kopp, J., and Schwede, T. (2006) *Bioinformatics* **22,** 195–201
27. DeFelice, L. J. (1981) in *Introduction to Membrane Noise* (DeFelice, L. J., ed) Plenum Press, New York
28. Garcia-Olivares, J., Alekov, A., Boroumand, M. R., Begemann, B., Hidalgo, P., and Fahlke, Ch. (2008) *J. Physiol.* **586,** 5325–5336
29. Fahlke, Ch., Yu, H. T., Beck, C. L., Rhodes, T. H., and George, A. L., Jr. (1997) *Nature* **390,** 529–532
30. Grewer, C., Gameiro, A., Zhang, Z., Tao, Z., Braams, S., and Rauen, T. (2008) *IUBMB Life* **60,** 609–619
31. Shachnai, L., Shimamoto, K., and Kanner, B. I. (2005) *Neuropharmacology* **49,** 862–871
32. Huang, S., and Vandenberg, R. J. (2007) *Biochemistry* **46,** 9685–9692
33. Ryan, R. M., and Mindell, J. A. (2007) *Nat. Struct. Mol. Biol.* **14,** 365–371
34. Vandenberg, R. J., Huang, S., and Ryan, R. M. (2008) *Channels* **2,** 51–58
35. Swenson, R. P., Jr., and Armstrong, C. M. (1981) *Nature* **291,** 427–429
36. Watzke, N., Bamberg, E., and Grewer, C. (2001) *J. Gen. Physiol.* **117,** 547–562
37. Raunser, S., Appel, M., Ganea, C., Geldmacher-Kaufer, U., Fendler, K., and Kühlbrandt, W. (2006) *Biochemistry* **45,** 12796–12805
38. Bouvier, M., Szatkowski, M., Amato, A., and Attwell, D. (1992) *Nature* **360,** 471–474